Internal free oscillations in Lake Ontario[1]

David J. Schwab

Great Lakes Environmental Research Laboratory, National Oceanic and Atmospheric Administration, Ann Arbor, Michigan 48104

Abstract

A numerical procedure is used to calculate some of the internal free modes of oscillation in a two-layer model of Lake Ontario, assuming a uniform equivalent depth. The modes fall into two categories, one set resembling Kelvin-type waves and the other resembling Poincaré-type waves. Observational evidence from Lake Ontario agrees qualitatively with the properties of these two types of modes.

During the summer the Great Lakes are stratified and exhibit long wavelength internal oscillations. Mortimer (1974) presented observations of several types of internal waves in the Great Lakes and showed that large-scale motions could be modeled well by linear shallow-water dynamics. Large-scale internal oscillations occur at discrete frequencies which depend on the physical dimensions of the lake. Knowledge of the discrete frequencies and associated structures of oscillations can help predict temperature and current variations in the stratified lake.

As a first approximation, a stratified lake is represented by two homogeneous layers of uniform depth and slightly different density. In this context the dynamics can be separated into two components, one corresponding to a completely homogeneous fluid—the barotropic part—and the other explicitly dependent on stratification—the baroclinic part. This separation reduces the system of six partial differential equations governing the two-layer dynamics to a much simpler system of three equations that can apply to either barotropic or baroclinic motion.

Kanari (1975) used the baroclinic equations to calculate the time dependent response of Lake Biwa to idealized wind stress. Harmonic analysis of time series from grid points in the model showed peaks at certain frequencies corresponding to the free internal modes of oscillation of the lake. The structures of the modes were determined from spectral amplitudes and phases. The results revealed an internal free oscillation resembling a Kelvin wave, which agreed with observed temperature oscillations in Lake Biwa.

The purpose of this study is to calculate explicitly the free baroclinic modes of oscillation of Lake Ontario. Stratification is represented by two discrete layers of uniform depth. A numerical procedure is applied to a finite difference grid approximating the shape of Lake Ontario. In this procedure the governing differential operators are discretized, and the frequencies and structures of the baroclinic normal modes are calculated numerically. The advantage of this approach is that the normal modes are determined explicitly, without recourse to time series analysis.

Rao and Schwab (1976) used this method to calculate the barotropic free oscillations of Lake Ontario. The three lowest modes have calculated periods of 5.11, 3.11, and 2.31 h. The lowest mode consists of a single amphidromic system with cyclonic phase progression (counterclockwise in the Northern Hemisphere). Higher modes exhibit an increasing number of amphidromes.

The present results for the baroclinic case show two distinct types of oscillation. One set resembles Kelvin waves with very low (subinertial) frequencies and cyclonic progression of phase. The other group has frequencies close to, but greater than, the inertial frequency and exhibits anticyclonic phase progression. These oscillations correspond, respectively, to Kelvin and Poincaré waves in a channel. Rao (1977) calculated the baroclinic modes of oscilla-

[1] GLERL Contribution 79.

tion in a rectangular basin and showed that the modes separate into these two distinct classes in basins large enough for the effect of the earth's rotation to be dominant. Observations of temperature and current oscillations in Lake Ontario support the existence of these two types of oscillations.

Method

The free response of a two-layer system can be separated into two independent components, one representing the motion of an equivalent homogeneous fluid (barotropic response) and the other characterized by nearly compensating volume transports in the upper and lower layer (baroclinic response). The method of separating the two components as given by Charney (1955) is exact only if the upper and lower layer equilibrium depths are constant. This approximation is used here as a first-order estimate of the stratification and bathymetry of Lake Ontario. The linearized equations governing the quasi-static barotropic and baroclinic motions in the absence of external forcing are

$$(\partial M/\partial t) - fN = -c^2(\partial\zeta/\partial x),$$

$$(\partial N/\partial t) + fM = -c^2(\partial\zeta/\partial y),$$

$$(\partial\zeta/\partial t) + (\partial M/\partial x) + (\partial N/\partial y) = 0. \quad (1)$$

Here M and N are the components of volume transport, ζ is surface elevation, c is the no-rotation wave velocity, and f is the coriolis parameter, twice the angular frequency of rotation. For the barotropic mode, M and N can be taken as transport components for the entire water column and ζ as the free surface displacement. In this case $c \equiv (gh)^{1/2}$ is the no-rotation phase speed of surface gravity waves. The gravitational constant is g, and the total depth is h. When these equations are applied to purely baroclinic motion, M and N are the lower layer transports and ζ is the displacement of the interface (*see* Csanady 1971). Phase speed for the baroclinic mode is $c \equiv (g^*h_e)^{1/2}$, where g^* is the gravitational constant reduced by the relative density difference between the two layers, and h_e is the equivalent depth of the two-layer system, the product of the individual layer depths divided by their sum. The boundary condition associated with Eq. 1 for both barotropic and baroclinic motions is that there be no transport normal to the shoreline.

Rao (1977) used a semianalytic procedure to solve Eq. 1 for a rectangular basin, but, in a basin of irregular geometry, the complicated shape prohibits the use of this technique. However, the basic theory can be cast into a numerical formulation in which the differential operators involved are discretized and applied to a grid representation of a lake. This numerical approach has been used to calculate the frequencies and structures of barotropic free oscillations in several lakes (Ontario and Superior: Rao and Schwab 1976; Michigan: Rao et al. 1976), but has not been applied to baroclinic oscillations. The parts of Eq. 1 governing baroclinic motions in the case of uniform equivalent depth have the same form as the equations solved in the references above, but the wave speed is greatly reduced. Details of the mathematical and numerical procedures for the solutions found below were explained by Rao and Schwab (1976).

The calculations of the free modes of oscillation governed by Eq. 1 proceed in three steps. The first two are numerical solutions for the eigenvalues and eigenvectors of two self-adjoint elliptic operators related to the irrotational and nondivergent parts of the flow field.

Step 1:

$$\nabla \cdot h\nabla\phi_a = -\lambda_a\phi_a$$

$$h(\partial\phi_a/\partial n) = 0 \quad \text{on the boundary.} \quad (2)$$

Step 2:

$$\nabla \cdot h^{-1}\nabla\psi_a = -\mu_a\psi_a$$

$$h^{-1}\psi_a = 0 \quad \text{on the boundary.} \quad (3)$$

These equations are discretized on a numerical grid, and the resulting standard eigenvalue problems are solved on a computer for the eigenvalues λ_a, μ_a and eigenvectors ϕ_a, ψ_a. The space dependent parts

Table 1. Calculated frequencies and periods of some internal oscillations of Lake Ontario.

Mode number	Frequency (cy s^{-1})	Period (h)	
1	2.92×10^{-6}	598	
2	5.86×10^{-6}	298	
3	8.73×10^{-6}	200	
4	1.17×10^{-5}	149	
5	1.44×10^{-5}	121	Kelvin-type
6	1.73×10^{-5}	101	oscillations
.	.	.	
.	.	.	
.	.	.	
25	8.95×10^{-5}	19.5	
26	9.75×10^{-5}	17.9	
27	9.97×10^{-5}	17.5	
- - - - - - - - - - - -			Inertial frequency
28	1.03×10^{-4}	16.9	
29	1.04×10^{-4}	16.8	
30	1.05×10^{-4}	16.7	Poincaré-type
31	1.06×10^{-4}	16.5	oscillations
32	1.07×10^{-4}	16.3	
33	1.08×10^{-4}	16.1	
.	.	.	
.	.	.	
.	.	.	

of the free solutions of Eq. 1 are then expanded in terms of ϕ_a and ψ_a to obtain

$$(M, N)^{\phi} = \sum_a p_a (M, N)_a^{\phi},$$

$$(M, N)^{\psi} = \sum_a q_a (M, N)_a^{\psi},$$

$$\zeta = \sum_a r_a \zeta_a, \qquad (4)$$

where $(M, N)_a^{\phi} = h\nabla\phi_a$, $(M, N)_a^{\psi} = \mathbf{k} \cdot \nabla\psi_a$, $\zeta_a = (\lambda_a/g)^{1/2}\phi_a$. Here $\mathbf{k}$ is the vertical unit vector.

The space dependent part of the transport field in Eq. 1 is the sum of the irrotational and nondivergent parts, i.e.

$$(M, N) = (M, N)^{\phi} + (M, N)^{\psi}.$$

The above expansions are substituted for (M, N) and ζ in Eq. 1, and the orthogonality of the ϕ_a and ψ_a functions allows isolation of the expansion coefficents (p_a, q_a, r_a). The final step in the process is to solve the resulting matrix eigenvalue problem for the frequencies (σ) of the free modes and corresponding expansion coefficient (p_a, q_a, r_a). The structures of the free modes are determined by evaluating the expansion for the height field ζ in Eq. 4. The complex variable ζ is represented in terms of amplitude and phase as

$$\zeta = A(x, y)\cos(\sigma t - \theta),$$

where

$$A(x,y) = (\mathrm{Re}\,\zeta^2 + \mathrm{Im}\,\zeta^2)^{1/2}$$

and

$$\theta = \arctan(\mathrm{Im}\,\zeta/\mathrm{Re}\,\zeta).$$

Results

The above method was used to solve Eq. 1 for a discretized model of Lake Ontario. Grid squares were 10.2 km on a side. The no-rotation wave velocity was chosen as $c = 43.4$ cm s^{-1}, corresponding to an upper layer depth of 15.6 m, lower layer depth of 70.4 m, and a relative density difference between layers of 1.50×10^{-3}. The expansions of dependent variables in Eq. 4 were limited by computer memory size to 80 functions each of the irrotational and nondivergent type. With this truncation, the calculation provided frequencies and structures of 80 internal normal modes.

As indicated in Table 1, the calculated frequencies separate into two categories which will later be identified as the enclosed basin analogues of Kelvin and Poincaré waves in a channel. The very low frequencies ($\sigma \ll f$) are all approximately integer multiples of the lowest frequency. In Fig. 1, structures of the three lowest frequency modes are presented in terms of the amplitude and phase distribution of the height field. Amplitude is normalized so that the maximum value is 100. The structure of the lowest mode in Lake Ontario shows maximum amplitude near the ends of the basin and cyclonic phase progression. Phase lines are somewhat spread near the ends of the basin, indicating a higher phase speed. The second and third lowest modes represent the same type of oscillation with ½ and ⅓ the longitudinal wavelength of the lowest mode. The frequencies of higher Kelvin-type modes increase as multiples of the lowest frequency. Their structures resemble oppositely propagating Kelvin waves in a channel with wavelengths of ½, ⅓, ¼, etc. of twice the

basin length. At some stage the structures become too complicated to resolve on the numerical grid, and the successive calculated frequencies no longer follow as strict multiples of the lowest. This continues until the frequency exceeds the inertial frequency, when suddenly the structures of the modes change to anticyclonic amphidromic systems with long wavelengths—the Poincaré-type modes.

The structure of the first mode with frequency higher than the inertial (not illustrated) is somewhat complicated, but it is dominated by anticyclonic phase progression. The next three modes (illustrated in Fig. 2) are Poincaré-type oscillations with maximum amplitude generally occurring on the north and south shores and with anticyclonic phase progression. Experience has shown that the series expansions in Eq. 4, used to determine the structures of the normal modes, converge most rapidly for the lowest frequencies. At the frequencies of the Poincaré-type oscillations, the convergence is not as rapid, and it was necessary to numerically smooth the calculated structures of the three modes in Fig. 2.

Discussion

Comparison with channel solutions—As Lake Ontario is an elongated basin, it is informative to describe some analytic solutions to Eq. 1 when applied to a channel. Some wave solutions for Eq. 1 are periodic both in time and in the long channel direction. The superposition of two such waves propagating oppositely in a rotating channel represents a quasi-standing wave, satisfying the boundary condition of vanishing normal transport at the channel sides, but retaining a nonzero normal transport component at the ends of the resulting cellular structures. Although each such superposition is not an exact solution for the free oscillations in a closed basin, certain linear combinations of the infinite number of them do satisfy the longitudinal boundary condition, thereby giving an exact solution to the closed basin problem. This principle was used by Taylor (1920) to model free oscillations in rectangular bays and basins. Starting with a pair of oppositely propagating Kelvin waves of equal wavelength, he was able to determine an infinite series of Poincaré waves which would exactly compensate for the nonzero longitudinal transport at transverse boundaries in the channel.

The character of the quasi-standing Kelvin wave is pictured in Fig. 3a in terms of amplitude, A, and phase, θ, for $f = 10^{-4}$ s^{-1}, $a = 30$ km (half-width), $c = 50$ cm s^{-1}, and wavenumber $k = \pi/10a$—values appropriate for the lowest baroclinic mode of this type in Lake Ontario. It is not a standing wave in the usual sense, since the longitudinal transports are nonzero at the ends of the cell. The main characteristics of the wave are the exponential decrease in amplitude away from the sides and the cyclonic progression of phase around an amphidromic point in the center of the cell. The lowest mode in Lake Ontario (Fig. 1a) does not exhibit as rapid a decrease in amplitude away from the shores and maximum amplitudes occur at the ends of the basin. In the numerical procedure applied to Lake Ontario, relative wave amplitude is calculated at grid square centers, which are all at least 5.1 km from shore. This grid resolution is sufficient to determine the oscillation frequencies and offshore structures of the modes, but in the nearshore zone the calculations may not show the initial rapid decrease in amplitude.

The elevation field of the simplest quasi-standing Poincaré wave is pictured in Fig. 3b in terms of A and θ with the values of f, a, c, and k used for the Kelvin wave. As with the Kelvin wave, longitudinal transport does not vanish at the ends of the cell. Apparent characteristics are the proximity of the frequency to the inertial frequency and anticyclonic progression of phase around the central amphidromic region. The frequency of the Poincaré wave associated with the chosen parameters is about 3% greater than the inertial frequency.

The frequency equation for Poincaré waves in a channel is (Defant 1961)

$$\sigma^2 = f^2 + c^2[(n^2\pi^2/2a) + k^2]. \quad (5)$$

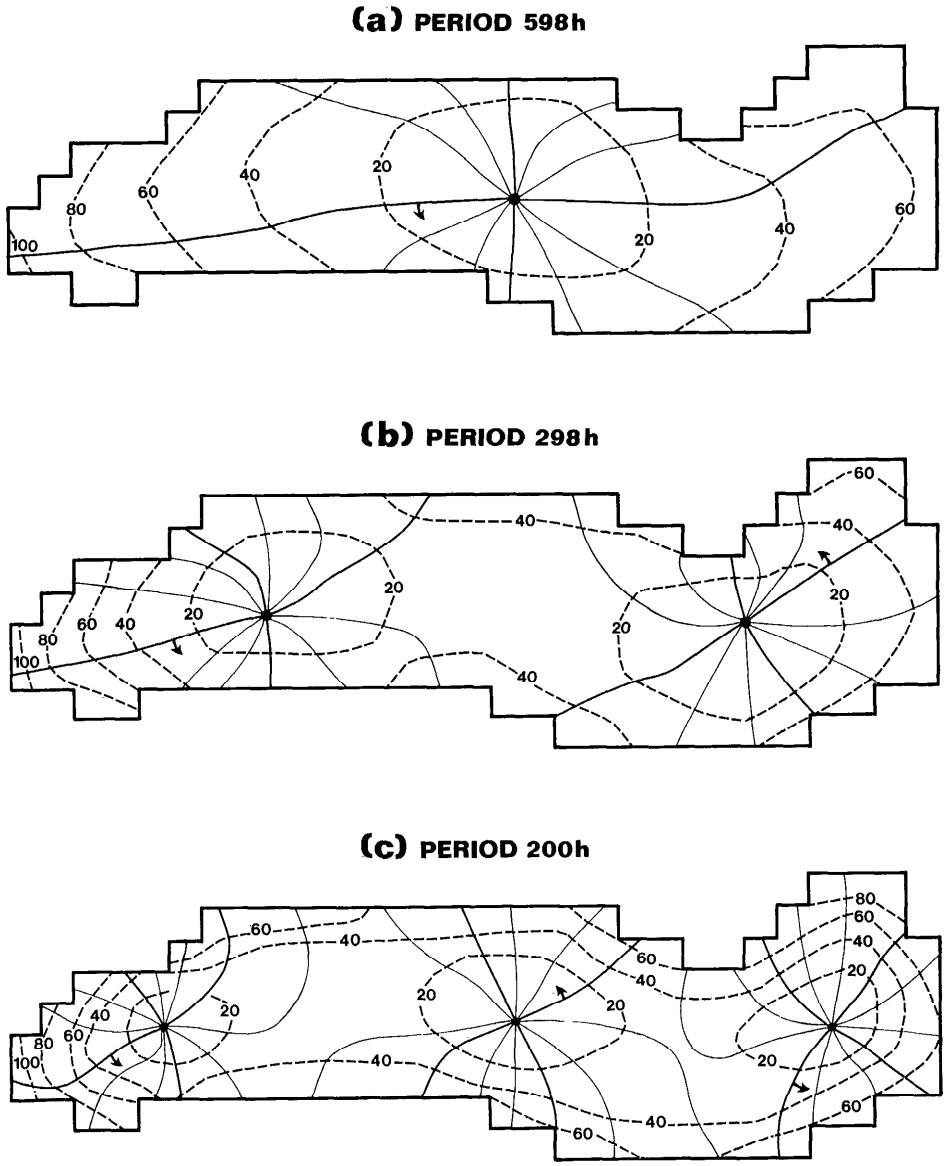

Fig. 1. Amplitude (% of max) and phase (in increments of 30°, 0° marked by arrow indicating direction of propagation) associated with three lowest calculated Kelvin-type modes in Lake Ontario.

Here n is an integer which represents the cross-channel nodality of the wave. The pictured Poincaré wave (Fig. 3b) is the simplest with $n = 1$. When $n = 2$, the structure consists of two amphidromic systems, each a distance $a/4$ from the channel sides. If the longitudinal wavenumbers of the calculated modes in Lake Ontario are taken as $k = \pi/L$, $2\pi/L$, $3\pi/L$, etc., the calculated frequencies correspond very well to Eq. 5.

Comparison with rectangular basin solutions—Although the Kelvin and Poincaré wave superpositions only approximate the standing wave pattern in a closed elongated basin, many of their characteristics can be

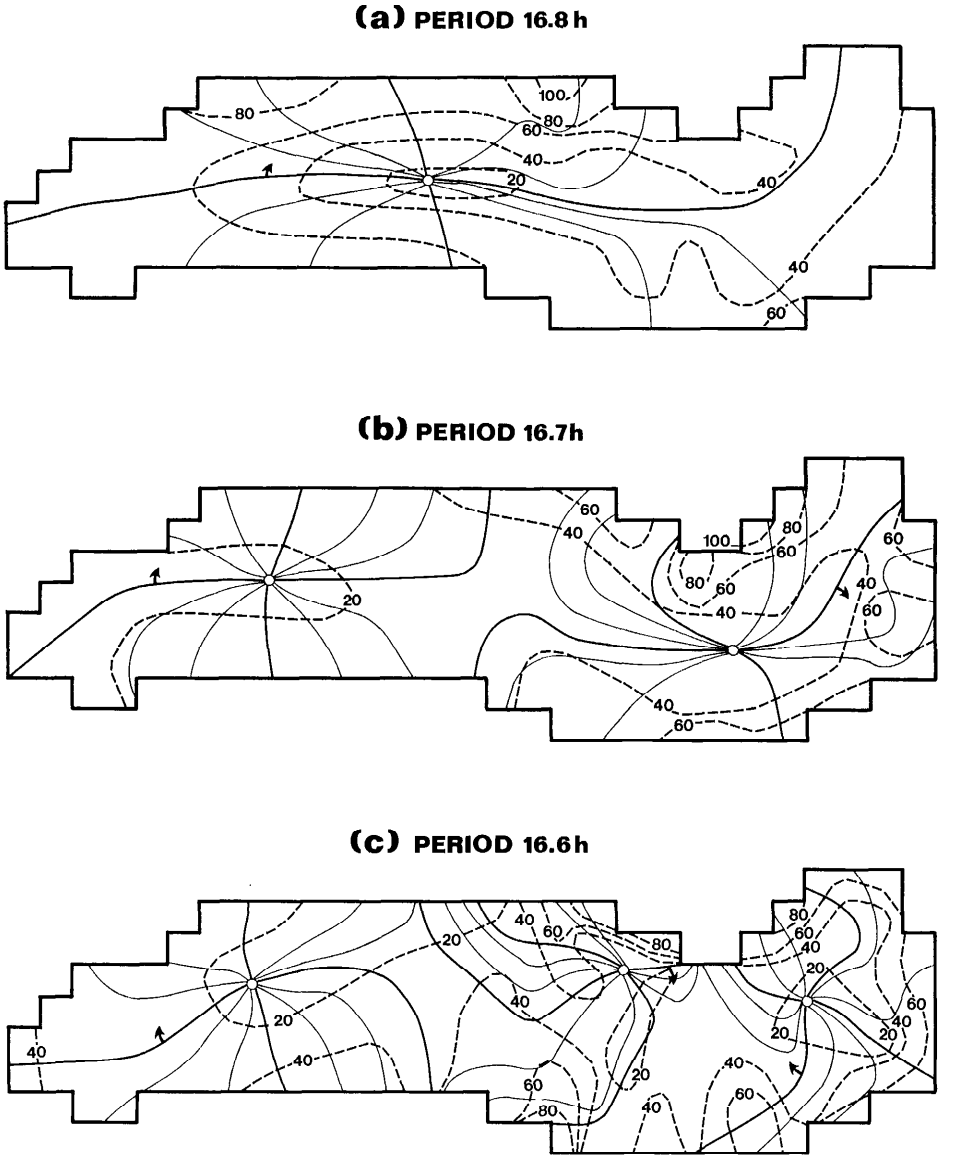

Fig. 2. Amplitude and phase distribution (as in Fig. 1) for three calculated Poincaré-type modes.

seen in the closed basin free modes of oscillation. Rao (1977) used a semianalytic method to calculate frequencies and structures of free internal oscillations in a rectangular basin. At nondimensional rotation rates corresponding to basin dimensions, wave speed, and rotation rate used above, the free oscillations separate into two classes, one set resembling oppositely propagating Kelvin waves, with low frequency ($\sigma \ll f$) and cyclonic progression of phase, and the other set resembling Poincaré waves, with frequencies very close to, but greater than, the inertial frequency and anticyclonic propagation of high water.

In the case of a channel, Kelvin waves

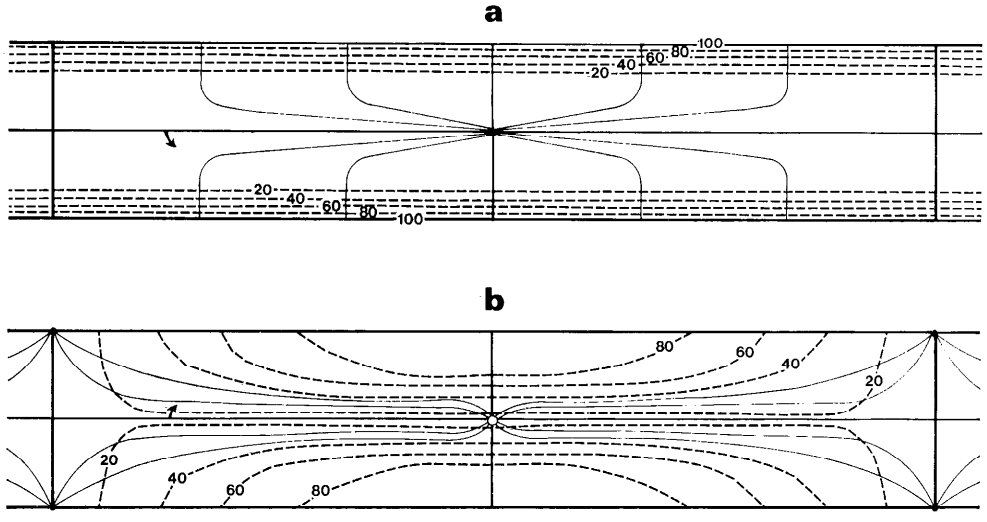

Fig. 3. Amplitude and phase distribution (as in Fig. 1) associated with the superposition of (a) two oppositely propagating Kelvin waves and (b) two oppositely propagating Poincaré waves.

have been shown to propagate at the no-rotation phase velocity c, implying a frequency for the quasi-standing Kelvin wave in Fig. 3a of $\sigma = \pi c/L$, where L is the length of the cell. The rectangular basin solution of Rao (1977) has a frequency 20% less than this value for parameters appropriate to Lake Ontario. The frequency of the lowest Kelvin-type mode in Lake Ontario is about 40% less than the channel frequency. The frequency is apparently decreased by the addition of transverse boundaries in the rectangular basin and further decreased by the irregular geometry of Lake Ontario.

It is somewhat surprising that the first calculated mode with frequency greater than the inertial is not the lowest Poincaré-type mode, but Rao's (1977) calculations in rectangular basins show similar results for certain basin dimensions and density differences. In his results for various nondimensional rotation rates, the frequency of a certain mode may be slightly greater than the inertial frequency but less than the frequency of the first Poincaré-type mode at one rotation rate and then become subinertial at higher rotation rates (corresponding to larger basin dimensions or decreased density difference). The structure of this type of mode is usually quite complicated when its frequency is in the vicinity of the inertial frequency.

Comparison with observations—Internal Kelvin-type waves have been observed in Lake Ontario by Csanady and Scott (1974) in two separate episodes during the 1972 International Field Year on the Great Lakes. They noted longshore current reversals and isotherm deflection associated with the crest of a wave propagating eastward along the south shore of the lake with an estimated propagation speed of 45 cm s^{-1}. The lowest Kelvin-type oscillation calculated here (*see Fig. 1a*) exhibits a propagation speed less than 45 cm s^{-1} at the shoreline near the middle of the lake (as low as 15 cm s^{-1}) and higher speed on the ends (as much as 75 cm s^{-1}) so that the average propagation speed is close to that estimated from observations. Such estimates are difficult because frictional dissipation decreases the amplitude of the wave, the thermal structure of the lake changes, and new storms interrupt the progress of a wave on this time scale. In view of these difficulties, the bracketing of the observed phase speed by the calculated minimum

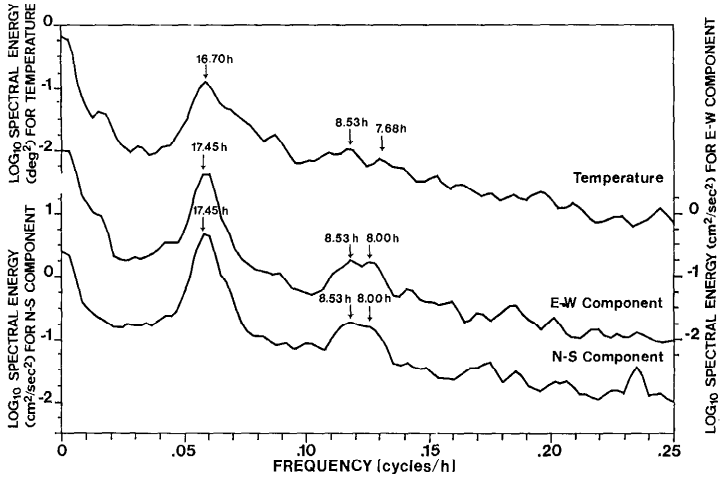

Fig. 4. Average power spectra of temperature, E–W current component, and N–S current component at 10-m depth during July 1972 (redrawn from Pickett and Richards 1975).

and maximum and the eastward propagation of the wave along the south shore represent only a qualitative verification.

Pickett and Richards (1975) presented horizontally averaged power spectra of temperature and current components at various depths in Lake Ontario for the month of July 1972 during the International Field Year for the Great Lakes. Three of the spectra (temperature, north-south current component, east-west current component at 10-m depth) are redrawn here in Fig. 4 with the spectral density scaled logarithmically so that some of the lower energy peaks are more conspicuous. As indicated in Table 1, the frequencies of the Poincaré-type modes are very close together in the range just above the inertial frequency. In order to separate the first and second modes at 1.03×10^{-4} and 1.04×10^{-4} cy s^{-1} by standard spectral analysis of temperature and current records, an uninterrupted record longer than the period of stratification in Lake Ontario would be required. Therefore, each of the frequency bands immediately above the inertial frequency in Fig. 4 probably contains energy from several modes so that only the gross distribution of energy can be examined.

The largest peak in the temperature spectrum is for the band centered at 16.70 h. Both current components show the greatest energy at 17.45 h, closer to the inertial period of Lake Ontario (17.35 h). Subsidiary peaks are seen in the temperature spectrum near the frequency of the semidiurnal tide and at periods of 8.53 and 7.68 h. In the current spectra there is not much energy at the tidal frequency but there are clear peaks in both current spectra at 8.53 and 8.00 h. The primary peak in the temperature spectrum is as close as possible to the period of the lowest Poincaré-type mode calculated here. The spectral energy in the temperature spectrum then trails off more slowly than in the current spectra at frequencies slightly higher than the inertial. The secondary peaks at 8.53 and 7.68 are at periods close to half the period of the lowest Poincaré-type modes with $k = \pi/L$ and $n = 1$ or $n = 2$ (in Eq. 5). The primary peak in the current spectra is closer to the inertial frequency than that of the lowest Poincaré-type node. The subsidiary peaks in the current spectra are closer to half the periods of the lowest Poincaré modes with $n = 1$ and $n = 2$ than half the inertial period. Mortimer (1971), examining similar secondary peaks in temperature and current spectra from Lake Michigan, suggested that the secondary peaks are the result of nonlinearities in the temperature and cur-

rent signals, causing increases in spectra amplitude at multiples of the fundamental frequency involved. The spectra in Fig. 4 then seem to show inertial currents not associated with oscillation of the thermocline, temperature and current fluctuations at periods just less than the inertial period, and the first harmonics of 17- and 16-h oscillations.

This evidence is consistent with the calculated periods and structures of the Poincaré-type modes. There is energy in several of the Poincaré-type modes with notably larger amounts in the $k = \pi/L$ and $n = 1$ or $n = 2$ modes. Since the periods of these modes are so close, limited spectral resolution does not permit separation of the fundamental frequencies, but the first harmonics show a clear split.

Conclusion

The calculated internal free oscillations of Lake Ontario fall into two categories. One group has frequencies much less than the inertial frequency and structures that resemble a pair of Kelvin waves propagating cyclonically around the shoreline. The frequency of the Kelvin waves is less than it would be in a channel, and the amplitude decreases more slowly away from shore. The other group is similar to quasi-standing Poincaré waves in a channel. The calculated frequencies are very close to, but always greater than, the inertial frequency. The frequencies can be predicted quite well by the frequency equation for Poincaré waves in a channel. The structures show anticyclonic phase progression. Observational evidence from Lake Ontario (Csanady and Scott 1974; Pickett and Richards 1975) agrees qualitatively with the properties of the two types of oscillation. The complication of depth variations, friction, and nonlinearities no doubt alter some of the characteristics of these modes, but the linear, frictionless theory used here provides a first approximation to the natural situation.

References

Charney, J. G. 1955. Generation of oceanic currents by wind. J. Mar. Res. **14**: 477–498.

Csanady, G. T. 1971. Baroclinic boundary currents and long edge-waves in basins with sloping shores. J. Phys. Oceanogr. **1**: 92–104.

———, and J. T. Scott. 1974. Baroclinic coastal jets in Lake Ontario during IFYGL. J. Phys. Oceanogr. **4**: 524–541.

Defant, A. 1961. Physical oceanography, v. 2. Pergamon.

Kanari, S. 1975. The long-period internal waves in Lake Biwa. Limnol. Oceanogr. **20**: 544–553.

Mortimer, C. H. 1971. Large-scale oscillatory motions and seasonal temperature changes in Lake Michigan and Lake Ontario. Univ. Wisconsin-Milwaukee, Center Great Lakes Stud. Spec. Rep. 12, Pt. 1 and 2.

———. 1974. Lake hydrodynamics. Mitt. Int. Ver. Theor. Angew. Limnol. 20, p. 124–197.

Pickett, R. L., and F. P. Richards. 1975. Lake Ontario mean temperatures and currents in July 1972. J. Phys. Oceanogr. **5**: 775–781.

Rao, D. B. 1977. Free internal oscillations in a narrow, rotating rectangular basin, p. 391–398. *In* T. S. Murty [ed.], Modeling of transport mechanisms in oceans and lakes. Proc. Symp. CCIW, Burlington, Ontario.

———, C. H. Mortimer, and D. J. Schwab. 1976. Surface normal modes of Lake Michigan: Calculations compared with spectra of observed water level fluctuations. J. Phys. Oceanogr. **6**: 575–588.

———, and D. J. Schwab. 1976. Two-dimensional normal modes in arbitrary enclosed basins on a rotating earth: Application to Lakes Ontario and Superior. Phil. Trans. R. Soc. Lond. Ser. A **281**: 63–96.

Taylor, G. I. 1920. Tidal oscillations in gulfs and rectangular basins. Proc. Lond. Math. Soc. Ser. 2 **20**: 148–181.

Submitted: 16 July 1976
Accepted: 10 January 1977